

1 Improving data acquisition speed and accuracy in sport using neural
2 networks

3 Christopher Papic^a, Ross H Sanders^a, Roozbeh Naemi^b, Marc Elipot^{c,d}, Jordan Andersen^a

4 ^aExercise and Sport Science, Faculty of Medicine and Health, The University of Sydney,
5 Australia

6 ^bSchool of Life Science and Education, Staffordshire University, United Kingdom

7 ^cSwimming Australia, Australian Institute of Sport Office, Canberra, Australia

8 ^dAustralian Analysis and Research Group for Optimisation in Swimming, Australia

9

10 Corresponding author

11

12 Christopher Papic

13 Email: chris.papic@sydney.edu.au

14 Twitter: [@chris_papic](https://twitter.com/chris_papic)

15 Abstract

16

17 Video analysis is used in sport to derive kinematic variables of interest but often relies on time-
18 consuming tracking operations. The purpose of this study was to determine speed, accuracy
19 and reliability of 2D body landmark digitisation by a neural network (NN), compared with
20 manual digitisation, for the glide phase in swimming. Glide variables including glide factor;
21 instantaneous hip angles, trunk inclines and horizontal velocities were selected as they
22 influence performance and are susceptible to digitisation propagation error. The NN was
23 'trained' on 400 frames of 2D glide video from a sample of eight elite swimmers. Four glide
24 trials of another swimmer were used to test agreement between the NN and a manual operator
25 for body marker position data of the knee, hip and shoulder, and the effect of digitisation on
26 glide variables. The NN digitised body landmarks 233 times faster than the manual operator,
27 with digitising root-mean-square-error of ~4-5mm. High accuracy and reliability was found
28 between body position and glide variable data between the two methods with relative error
29 $\leq 5.4\%$ and correlation coefficients > 0.95 for all variables. NNs could be applied to greatly
30 reduce the time of kinematic analysis in sports and facilitate rapid feedback of performance
31 measures.

32

33 Keywords

34

35 Swimming, digitisation, video analysis, performance analysis, applied biomechanics

36 Introduction

37

38 Video footage is commonly used to analyse human movement and performance in training and
39 simulated competitive sporting environments. Kinematic analysis of video involves the
40 identification of body landmark positions (e.g. joint centres) through the process of
41 'digitisation' to obtain pixel coordinates for each frame of video data. These coordinates are
42 converted to real world metric positions and are used to derive kinematic variables of interest.
43 Digitisation of video data in sport is commonly performed manually, where an operator
44 estimates the position of joint centres without the need for external markers on the athlete.
45 Manual digitisation, however, is not conducive to time-efficient performance analysis and
46 feedback, nor for analysing large datasets, due to its laborious nature.¹ Video analysis software
47 with image recognition algorithms can automate digitisation of body landmarks in video;
48 however, some systems require manual intervention to improve digitisation accuracy to an
49 acceptable level,² limiting the amount of time saved. In contrast, accuracy is sometimes
50 sacrificed to increase processing speeds; for example, calculations of 2D knee angle during a
51 drop jump from body landmark data, digitised by automatic digitising software, produced a
52 considerable range of error (0.21-37.93%) compared to 'a gold-standard' optoelectric motion
53 capture system.³ There seems to be a trade-off between accuracy and processing time with
54 video analysis software, leaving users with the decision of what to sacrifice.

55 Neural networks (NNs) are proven to be highly accurate and time-efficient for image
56 recognition tasks when sufficiently trained on a large dataset.⁴ For example, 10,500 images of
57 subjects performing lifting tasks were used to train a NN to automatically digitise multiple 3D
58 joint positions, based on annotated body landmark position data derived from an optoelectric
59 motion capture system.⁵ Mean 3D landmark position error between the NN and the motion
60 capture system was $14.72 \pm 2.96\text{mm}$, highlighting the potential for automatic digitisation of
61 video data using NNs. The NN design, however, was limited by the requirement of a motion
62 capture laboratory to train the NN. Through a process called 'transfer learning', image
63 recognition abilities of an existing NN are used to develop a new NN to recognise features in
64 images, such as body landmarks, that the initial NN has not digitised previously. The advantage
65 of this approach is that standard video analysis and manual digitisation procedures can be used
66 to train a NN, which may be more viable for sport scientists working with athletes in training
67 and simulated competitive environments. For instance, the NN software DeepLabCutTM utilises
68 transfer learning and an image feature detection algorithm^{4,6,7} to 'learn' user-defined features

69 in a relatively small number of training images (<500) and digitise similar features in new
70 videos.

71 NNs may be particularly advantageous for kinematic analysis in aquatic environments,
72 which poses added methodological challenges. Manual digitisation in swimming research, for
73 example, is necessary to minimise body landmark position error and missed landmarks by
74 automatic methods since the identification of markers can be affected by turbulence, air
75 bubbles, and vortices that can obscure the markers.⁸ Cronin et al.⁹ demonstrated that a NN
76 could be used to digitise 2D joint positions during underwater running with comparable
77 accuracy to a manual operator. NNs could provide a faster alternative to manual digitisation of
78 body landmarks in aquatic video data.

79 The use of video analysis in swimming is practical for movement and performance analysis
80 because swimmers' motion can be captured without manipulating technique.¹⁰ Video analysis
81 is often used to analyse the glide component of the underwater phase of start and turns because
82 start time and overall swimming performance are highly dependent on the glide.^{11,12} Glide
83 performance is influenced by the swimmer's ability to minimise hydrodynamic resistance and
84 deceleration during the glide (e.g. glide efficiency) and to maintain posture during the glide
85 (e.g. hip angle¹³ and trunk incline¹⁴). Given the glide remains predominantly in the sagittal
86 plane, digitisation of body landmarks in 2D video can be used to derive glide efficiency,
87 posture, and performance outcome measures. Deriving these measures from 2D position data,
88 however, can amplify the magnitude of digitisation error, evidenced when calculating the first
89 derivative of position data.¹⁵ While markerless 2D joint position error between manual and NN
90 digitisation methods in an aquatic setting may be acceptable,⁹ the effect of digitisation error on
91 kinematic outcomes of the glide, such as velocity and glide efficiency, requires further
92 investigation. Athletes and coaches would benefit from an accurate and time-efficient method
93 for glide analysis.

94 The emerging use of NNs for image feature detection may be applicable to kinematic
95 analysis in sport to improve data acquisition speed and accuracy. The purpose of this study was
96 to train a NN to digitise body landmarks in 2D video of athletes in a sporting environment and
97 to compare the time, accuracy, and reliability of digitisation and derived kinematic variables
98 by the NN with manual digitisation.

99

100 Method

101

102 Participants

103

104 Five male (age: 21.6 ± 2.1 years, height: 187.72 ± 7.61 cm, mass: 85.68 ± 2.80 kg, FINA
105 score: 677 ± 53.9) and four female (age: 20.3 ± 2.1 years, height: 172.03 ± 6.42 cm, mass:
106 68.98 ± 8.61 kg, FINA score: 723.5 ± 85.7) state and national level swimmers from an Australian
107 swimming club were recruited. FINA point scores were calculated for the swimmers' 100m
108 long course best time of their preferred stroke within the previous 12 months. The swimmers
109 were informed via a printed participant information statement and gave their free written
110 consent to take part in the study.

111

112 Procedures

113

114 The testing procedures were conducted for a subsequent study to evaluate the effects of
115 verbal cuing on glide performance. Data collection was conducted in a ten-lane 25m pool (3m
116 depth). Swimming training attire was worn to expose the greater trochanter for body marking:
117 briefs for males and one-piece swimsuit for females. Height and body mass were taken using
118 a stadiometer and electronic weight scale (WS207PMSG, Wedderburn, Australia). Body
119 landmarks were marked using black 'ProAiir Hybrid' waterproof body paint (Face Paint Shop
120 Australia, Yamba) with 4cm diameter circles.¹⁶ The following body landmarks were marked
121 on the lateral aspect of the swimmers' right side: knee joint axis, hip over the greater trochanter,
122 and shoulder over the glenohumeral joint at C7 height. The landmarks were identified by an
123 Accredited Exercise Physiologist (Exercise & Sports Science Australia) while the swimmer
124 adopted a streamlined position standing on the pool deck.

125

126 Swimmers performed underwater glides from the wall in the streamlined body position
127 without upper or lower limb actions; where the arms were extended forward above the head,
128 the hands pronated and overlapping, and the feet plantarflexed and positioned together.¹⁷
129 Swimmers attempted glides until they achieved ten successful trials. A glide was deemed
130 successful when the swimmer maintained a horizontal body position and trajectory without
lateral deviation from the black lane line, which was assessed visually by two researchers.

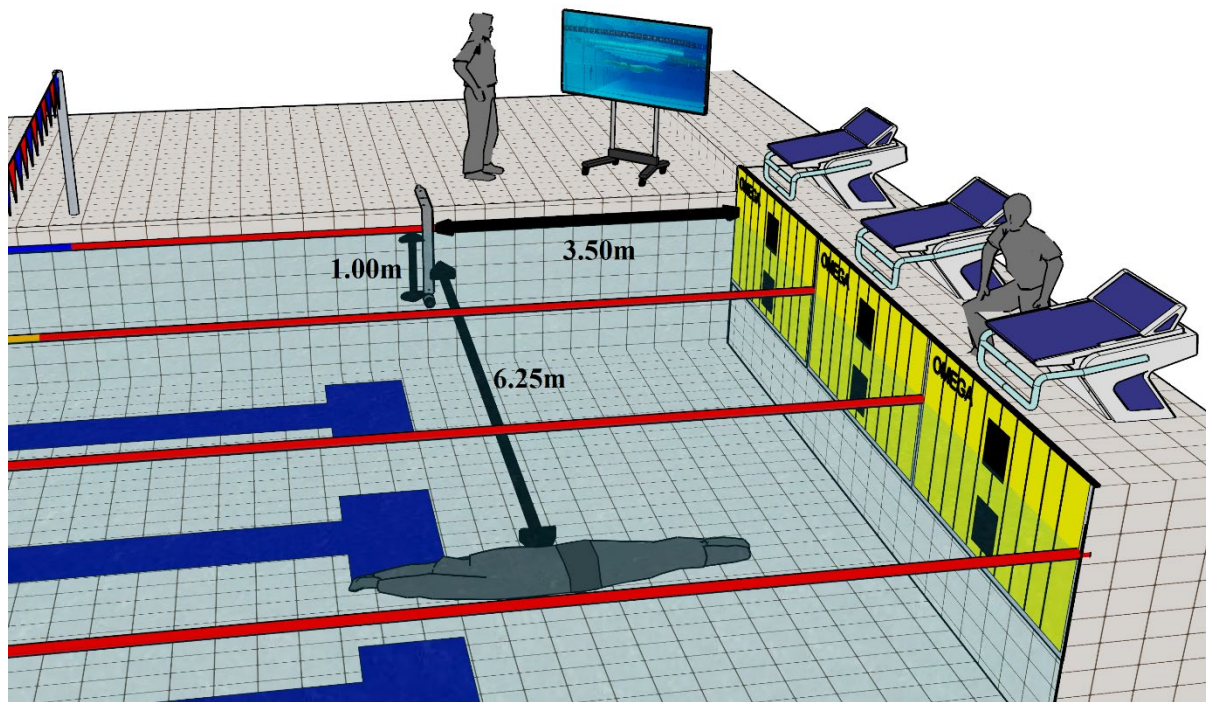
131

132 Data acquisition

133

134 A visual representation of the experimental setup is illustrated in Figure 1. A SwimPro
135 X underwater camera system (SwimPro RJB Engineering, Australia) captured the swimmers'
136 glides as they pushed off the start wall. The underwater camera was located 3.5m from the start
137 wall in the lane closest to the side of the pool at a depth of 1.0m, such that the camera was
138 positioned 6.25m perpendicular to the direction of the swimmers' motion. The camera was
139 fixed with a wall mount and recorded video at 30Hz and capture resolution of 1920x1080
140 pixels. Video data were transmitted wirelessly from the camera to a computer located on the
141 pool deck via an antenna connected to the underwater camera by a waterproof cable. The
142 SwimPro software (SwimPro RJB Engineering, Australia) displayed the recordings in real time
143 and saved each glide in mp4 format. Glide trials were captured with the swimmer moving from
144 left to right of the capture screen, with the knee, hip, and shoulder landmarks on the right side
145 of the body visible for kinematic analysis.

146



147

148

Figure 1. Experimental setup for 2D glide analysis

149

150 Data analysis

151

Video processing

The 'Cinalysis' software¹⁸, was used to process the videos. Fisheye distortions were removed using checkerboard calibration (9x7, 29mm squares) as defined by Bouguet.¹⁹ The camera lens was modelled using three coefficients to represent radial distortions and two to represent the tangential distortions, derived from the extracted corner points and known size of the checkerboard pattern.²⁰ Each glide trial was then trimmed and exported as 105-frame corrected glide trials: 45-frames to analyse the glide with 30-frames buffer before and after. The first frame of the glide to be analysed was when the swimmer achieved the streamlined position after leaving the wall. A calibration plane (4.98x1.00m) containing 40 calibration points, covering the entire underwater zone of interest, was used to compute the calibration coefficients applying a 2D direct linear transformation method.²¹ The calibration error was assessed as the reprojection error, defined by Kwon and Casebolt,²² where root-mean-square error (RMSE) of the reconstructed calibration marker positions were 4.7mm and 4.9mm for the x- and y-axis coordinates, respectively.

Manual digitisation

Four glides from a single swimmer were used to assess the accuracy of digitisation by the NN against manual digitisation. The four glide trials consisted of 420-frames of video data, with 1260 available body landmarks (knee, hip, and shoulder). Manual digitisation of these four glide trials was completed five times by the first author using the graphical user interface within the DeepLabCutTM software. Digitisation was performed across multiple days and the same glide trial was never re-digitised on the same day to ensure reliability was not affected by practice.⁸ X- and y-pixel coordinates of the five repeated manual digitisations were averaged for each landmark in each frame of data in the four trials. The coordinates were averaged to define the most likely manually derived position for a given landmark. These data were used to evaluate the accuracy and reliability of digitisation by the NN against the manual operator.

Neural network training and digitisation

DeepLabCutTM (v2.1) was used to train a NN to digitise the knee, hip, and shoulder. Four hundred frames (following recommendations from Cronin et al⁹) were randomly

185 extracted, using the k -means algorithm in DeepLabCutTM, from glides performed by eight
186 participants to train the NN. The four glide trials from the remaining participant (i.e. the trials
187 used to assess the accuracy of the NN against manual digitisation) were excluded from the
188 training process. The remaining six glides from this participant were set aside and digitised by
189 the NN as part of the complete data set, as described below. The last author manually digitised
190 the three landmarks in all 400 training frames. Inter-rater reliability between the first and last
191 author was tested using a separate database of glide videos (see *Manual digitisation reliability*).

192 Image feature learning by a NN involves calculating the probability, known as a
193 ‘weight’, that there is a match between the red-green-blue (RGB) characteristics for a region
194 of an image, known as the ‘input’, and the RGB characteristics of the region surrounding a
195 body landmark, referred to as the user-defined ‘ground truth’. With transfer learning, training
196 time is significantly reduced since a set of weights previously trained to identify RGB
197 characteristics in a very large image database are used as a starting point for a new NN. Training
198 by transfer learning involves updating the pre-trained weights by comparing the input with the
199 ground truth for new images.

200 Initial weights pre-trained on ImageNet²³ served as a starting point to train the NN for
201 200,000 iterations using the ResNet-50 architecture in DeepLabCutTM.⁴ A 0.95 training fraction
202 was used for the train/test ratio, meaning 95% of the 400 training frames were used to train the
203 NN and 5% were used to assess the network’s accuracy in estimating pixel coordinates of the
204 body landmarks. The mean test error (that is, the output of the ‘loss function’) was calculated
205 as the average difference between the pixel coordinates from manual digitisation (i.e. the
206 ground-truth) and the NN’s estimations.

207 The NN was trained in Google Colaboratory on a virtual 13Gb Tesla P100 GPU
208 (CUDA v10.1). The weights were saved to a basic local machine containing a 7th Gen Intel
209 Dual Core i5-7300 CPU (2.6GHz) with 8Gb of memory. Glide videos (n=90) from all
210 participants were then processed on the local machine in DeepLabCutTM using the trained NN
211 to digitise the body landmarks. The NN software output estimations for the raw x- and y-pixel
212 coordinate of each body landmark and the probability of these estimations for every frame. The
213 probability that a body landmark exists at a given pixel was calculated for each pixel on what
214 is called a ‘score-map’.²⁴ A score-map was generated for every landmark in each image of a
215 video during processing. The location of each body landmark was determined as the pixel with
216 the maximum probability on the score-map for that image.⁴

217

219

220 Kinematic data were calculated using coordinate data digitised by the manual operator
 221 and the NN from the four glide videos excluded from the training process. It is critical to note
 222 that the NN had never “seen” these images and therefore the robustness of the NN in this test
 223 setting could be evaluated. Figure 2 summarises the glide data processing stages following
 224 manual and NN digitisation of the four trials. After digitisation, raw pixel coordinate data were
 225 transformed into position data (mm) using the calibration coefficients described in the *Video*
 226 *processing* section. A cubic spline filter was used to interpolate missing data points, producing
 227 filled position data.

228 Glide efficiency is the ability of the swimmer to minimise deceleration during the glide
 229 and is reflected in a ‘glide factor’ obtained by curve-fitting 2D position data of body landmarks
 230 with a function based specifically on hydrodynamic principles.²⁵ Glide factor (m) was
 231 calculated using the hydro-kinematic method²⁵ in MATLAB for the 45 glide frames in each of
 232 the four glide trials. Filled position data were used to calculate glide factor to avoid over
 233 filtering. The mean position of the knee, hip, and shoulder for each frame were used to calculate
 234 glide factor due to better accuracy than using a single body landmark.^{25,26} Logarithmic fitting
 235 was done by solving the differential equation of horizontal glide motion, where x is the x-axis
 236 instantaneous filled position data, C_G is glide factor, and V_{xo} is the initial velocity (Equation 1).
 237 C_G was solved using Equation 1 to determine the glide factor for each of the four glide trials.

238

$$239 \quad x = C_G \cdot \ln \left[\frac{V_{xo}}{C_G} \cdot t + 1 \right] \quad (1)$$

240

241 A 4th order Butterworth low-pass filter with a 6Hz cut-off frequency was applied to the
 242 105-frames of filled position data. The 45-frames of filled and filtered position data from each
 243 of the four glides were used to calculate the following glide performance variables for each
 244 frame: horizontal velocity along the x-axis (m/s), hip angle (°), and trunk incline (°). Horizontal
 245 velocity was calculated to assess the amplified effect of digitising error on the first derivative.¹⁵
 246 Horizontal velocity (v) was calculated separately for the hip, knee, and shoulder using forward
 247 differentiation of the position data (x , m) with respect to time (t , seconds) for each frame (i)
 248 (Equation 2).

249

$$250 \quad v_i = \frac{x_{i+1} - x_i}{t_{i+1} - t_i} \quad (2)$$

251

252 Hip angle was the angle of the swimmer's right thigh with respect to the trunk. The
253 positions of the knee (k_x, k_y), hip (h_x, h_y), and shoulder (s_x, s_y) were used to determine distances
254 between hip and shoulder (d_{hs} , cm), hip and knee (d_{hk} , cm), and knee and shoulder (d_{ks} , cm).
255 The distance calculation is shown in Equation 3 using the hip and shoulder as an example and
256 was repeated for the other distances. Hip angle (θ , °) was then calculated using these distances
257 for each frame (Equation 4).

258

$$259 \quad d_{hs} = \sqrt{(s_x - h_x)^2 + (s_y - h_y)^2} \quad (3)$$

260

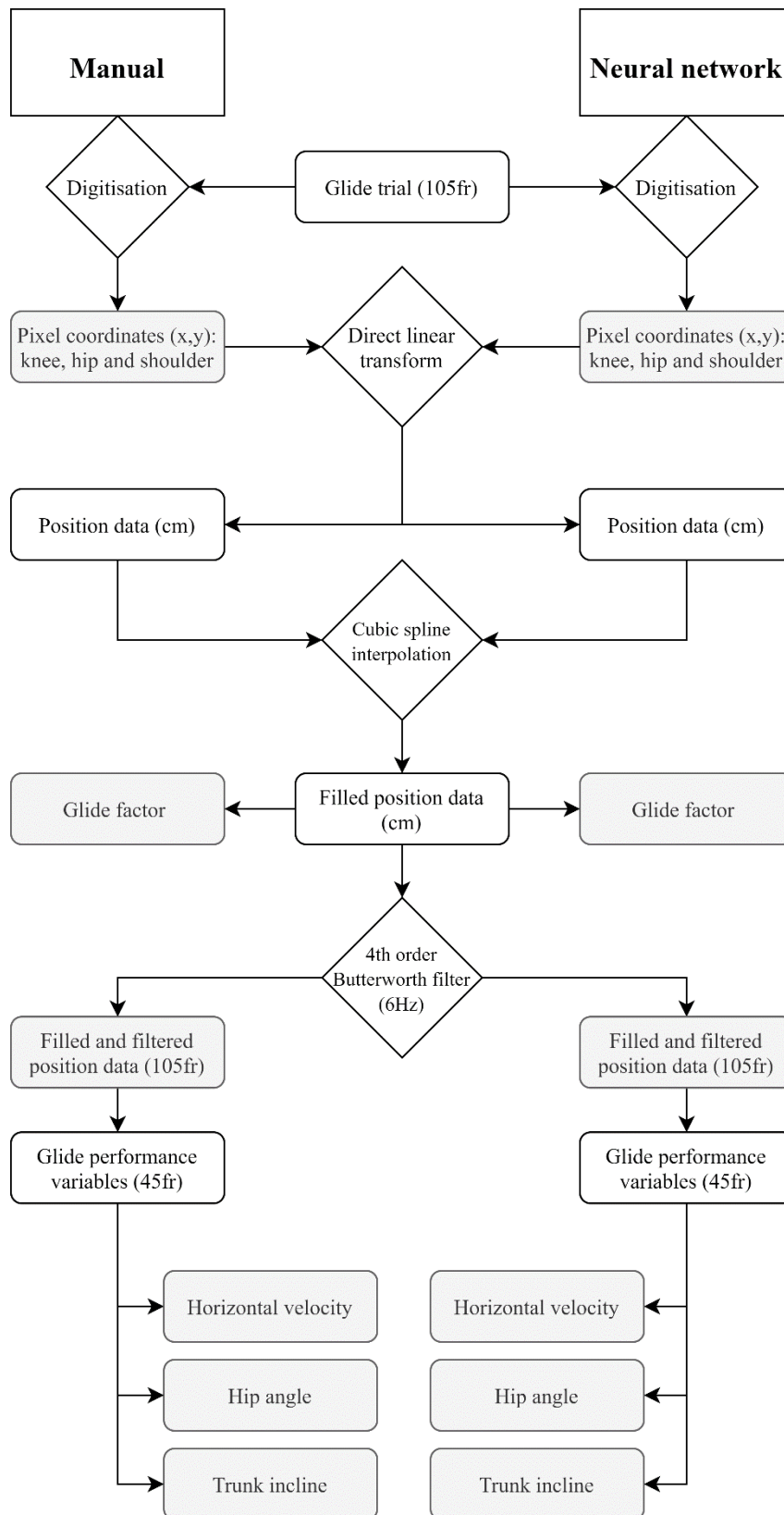
$$261 \quad \theta = \frac{180}{\pi} \cos^{-1} \frac{(d_{hs}^2 + d_{hk}^2 - d_{ks}^2)}{2 \cdot d_{hs} \cdot d_{hk}} \quad (4)$$

262

263 Trunk incline (φ , °) was calculated as the angle between the trunk, defined by the hip
264 and shoulder position data, and the external x-axis (Equation 5).

265

$$266 \quad \varphi = \frac{180}{\pi} \tan^{-1} \frac{(s_y - h_y)}{(s_x - h_x)} \quad (5)$$



267
 268
 269
 270
 271

Figure 2. Data processing procedures of manual and neural network kinematic analysis of the glide phase. Accuracy and reliability analysis procedures described in “*Statistical analysis: neural network versus manual digitisation*” were carried out for the tabs shaded in grey.

272 Statistical analysis

273

274 Statistical analysis was performed using SPSS (Version 25, SPSS Inc., Chicago, USA),
275 unless otherwise specified. Statistical significance was accepted at $p < 0.05$ for all tests. For all
276 intra-class correlation calculations, an absolute agreement, two-way mixed effects ICC model
277 was used.²⁷ ICC values less than 0.5, between 0.5 and 0.75, between 0.75 and 0.9, and greater
278 than 0.90 were indicative of poor, moderate, good, and excellent reliability, respectively.²⁷

279

280 *Manual digitisation reliability*

281

282 Intra-rater reliability for the first author's five digitisation attempts of the four glide
283 trials was assessed using ICCs of raw pixel x- and y-coordinates of the body landmarks. Using
284 Microsoft Excel, the mean of the standard deviations (mean error) of five digitisation attempts
285 of the four glide trials (i.e. 20 datasets) were calculated for the time series data of horizontal
286 velocity; hip angle; trunk incline; and glide factor. Ninety-five percent confidence intervals
287 (95% CIs) were calculated for each of these variables using the *t*-distribution and the mean
288 error. The confidence intervals were applied to the mean of each variable across the four trials
289 to produce an acceptable range from five repeated digitisation attempts by a human operator.
290 Inter-rater reliability of manual digitisation between the first and last authors was evaluated
291 using RMSE and ICCs for 214-frames from ten pilot glide trials (approximately 20 random
292 frames per trial) recorded using the same procedures in this study.

293

294 *Neural network versus manual digitisation*

295

296 Average time taken by the manual operator to digitise a single trial was calculated. The
297 time to train the NN and the time required by the NN to digitise all trials (n=90) were also
298 recorded. Similarity between digitisation by the manual operator and by the NN was assessed
299 with RMSE and ICC for raw pixel coordinate data (x- and y-axis); filled and filtered position
300 data (x- and y-axis); and instantaneous horizontal velocities, hip angles, and trunk inclines
301 across the four trials (see Figure 2). RMSE was also calculated for glide factor. Relative error
302 (%) of the RMSE for instantaneous velocities, hip angle, trunk incline, and glide factor were
303 calculated by dividing the RMSE by the range (maximum-minimum) of each variable across
304 the four trials and multiplying by 100. To evaluate the effect of glide velocity on digitisation

305 accuracy, relative error (%) of the RMSE for NN and manually derived instantaneous velocities
306 were calculated for all body landmarks (n=4 glides) within the manually derived glide velocity
307 ranges: <1.4m/s, 1.4-1.6m/s, 1.6-1.8m/s, 1.8-2.0m/s, 2.0-2.2m/s, and >2.2m/s. Instantaneous
308 velocity error was used to evaluate the effect of glide velocity on digitisation accuracy due to
309 the susceptibility of error inflation when calculating the first derivative. 95% CIs were used to
310 determine whether the neural network-derived means fell within an acceptable range of the
311 human operator-derived average value for each variable.

312 Results

313

314 Manual digitisation reliability

315

316 Intra-rater reliability was ‘excellent’²⁷ between digitisation attempts by the first author
317 for all body landmarks in each of the four glide trials (x-coordinates: ICC=1.00, $p<0.001$ and
318 y-coordinates: ICC>0.99, $p<0.001$). Inter-rater reliability was ‘excellent’ for digitisation
319 conducted by the first and last authors for all body landmarks (x-coordinates: ICC>0.99,
320 $p<0.001$ and RMSE=0.50 pixels; y-coordinates: ICC>0.99, $p<0.001$ and RMSE=0.45 pixels).

321

322 Neural network versus manual digitisation

323

324 The NN was trained in Google Colaboratory over approximately nine hours, without
325 the need for monitoring by a human operator, producing a mean test error of 2.04 pixels, or
326 5.7mm. The NN digitised 90 glide videos consisting of 105-frames each (28,350 body
327 landmarks) in 13.5min on the basic local machine. Average time for the first author to digitise
328 a single 105-frame glide trial (315 body landmarks) was approximately 35min.

329 Frames containing body landmarks that were unidentifiable due to image blurring or
330 that were obscured by air bubbles were omitted from analysis. Landmarks that were labelled
331 with <95% probability by the NN were also omitted. Post-hoc analysis of the landmarks
332 omitted from manual digitisation were found to be the same as those that were assigned <95%
333 probability by the NN. Consequently, 3.8%, 14.5%, and 4.5% of knee, hip, and shoulder body
334 landmarks, respectively, were filled using a cubic spline filter. Comparisons of position data
335 between manual and NN digitisation are shown in Table 1. Agreement in raw pixel and filled
336 and filtered position data for knee, hip, and shoulder in the x- and y-axis between the two

337 methods was near perfect ($ICC > 0.999$, $p < 0.001$). RMSE of position data for all body
 338 landmarks was approximately 4-5mm.

339

340 **Table 1.** Comparison of digitised x- and y-coordinate and position data by manual and neural
 341 network digitisation.

Variable	Knee			
	x		y	
	RMSE [†]	ICC [‡] , <i>p</i>	RMSE	ICC, <i>p</i>
Raw coordinate (pixel)	1.78	>0.999, <0.001	1.77	>0.999, <0.001
Filled and filtered position (mm)	5.2	>0.999, <0.001	4.7	>0.999, <0.001
	Hip			
	x		y	
	RMSE	ICC, <i>p</i>	RMSE	ICC, <i>p</i>
Raw coordinate (pixel)	2.06	>0.999, <0.001	1.50	>0.999, <0.001
Filled and filtered position (mm)	5.1	>0.999, <0.001	3.9	>0.999, <0.001
	Shoulder			
	x		y	
	RMSE	ICC, <i>p</i>	RMSE	ICC, <i>p</i>
Raw coordinate (pixel)	1.91	>0.999, <0.001	1.62	>0.999, <0.001
Filled and filtered position (mm)	4.8	>0.999, <0.001	4.0	>0.999, <0.001

342 †Root-mean-square error; ‡Intra-class correlation coefficient

343

344 Means, standard deviations, and 95% CIs of each glide performance variable and
 345 comparisons of glide performance variables derived from manual and NN digitisation are
 346 shown in Table 2. ‘Excellent’ reliability ($ICC > 0.95$, $p < 0.001$) was found in all glide
 347 performance variables, with relative error $\leq 5.4\%$. Mean glide variables from the four trials
 348 derived by the NN were within the acceptable range of the manual operator. Since glide factor
 349 was determined from a single swimmer, glide factor relative error was calculated using the
 350 range in glide factor (4.17–5.24 m) from a sample of 16 elite swimmers²⁸ of similar ability to
 351 our swimmer. Digitisation accuracy between the NN and manual operator decreased as glide
 352 velocity increased, with greater relative instantaneous velocity error at higher glide velocities
 353 (Figure 3).

354

355

356

357

358

359

360

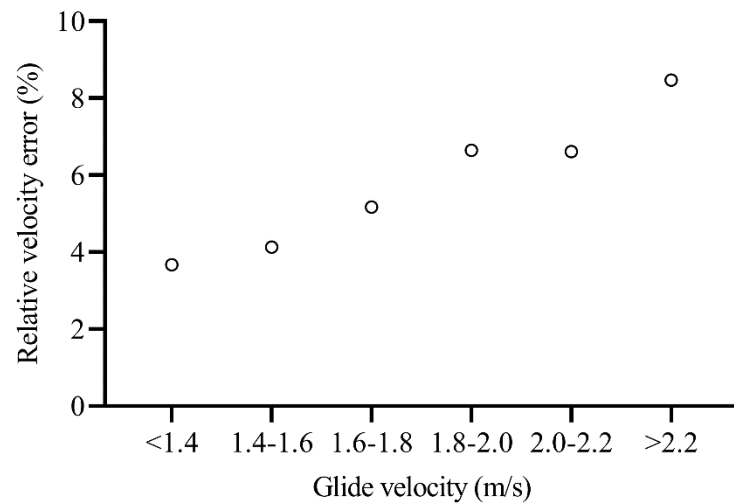
361

362 **Table 2.** Comparative analysis of glide performance variables derived by manual and neural
 363 network digitisation.

Glide variable	Manual mean trials=4	Intra-rater 95% CIs [†] trials=4 of n=5 repeats	Neural network mean trials=4	Mean difference	Manual vs neural network (RMSE [‡])	Relative error (%)	ICC [§] , <i>p</i>
Knee velocity (m/s)	1.76	1.70-1.85	1.77	0.01	0.10	5.4	0.977, <0.001
Hip velocity (m/s)	1.81	1.73-1.89	1.81	<0.01	0.09	4.8	0.982, <0.001
Shoulder velocity (m/s)	1.81	1.74-1.87	1.81	<0.01	0.08	4.4	0.984, <0.001
Hip angle (°)	166.00	164.50-167.50	166.13	0.13	0.73	3.7	0.996, <0.001
Trunk incline (°)	1.59	1.42-1.77	1.64	0.05	0.28	3.5	0.998, <0.001
Glide factor (m)	4.80	4.64-4.97	4.82	0.02	0.03	2.9	-

364 [†]Ninety-five percent confidence intervals; [‡]Root-mean-square error; [§]Intra-class correlation coefficient

365



366

367 **Figure 3.** The effect of glide velocity on instantaneous velocity error (relative error of the
 368 root-mean-square error, %), derived from NN and manually digitised body landmarks.

369

370 Discussion

371

372 The purpose of this study was to determine the speed, accuracy and reliability of a NN
 373 to digitise body landmarks in 2D videos against manual digitisation and to assess accuracy and
 374 reliability of the derived kinematic variables from those body landmark data. The performance
 375 of the NN trained in DeepLabCutTM exceeded expectations. Not only were the relative errors
 376 within the bounds of manual digitisation (Tables 1 and 2), the NN digitised video data at a rate
 377 *233 times faster than the manual operator*. By comparison, automated digitisation methods
 378 with corrective manual adjustments have improved digitising time by 2.5 times that of manual

379 digitisation.^{2,29} In addition to significant improvements in digitising time, position data
380 digitised by a NN can be used to compute movement and performance variables with high
381 accuracy and reliability compared with manually-derived variables (Table 2). The findings
382 have implications for applying NNs to digitise video data in biomechanics research to enable
383 accurate and expedient performance analysis.

384

385 Comparison of the neural network with existing digitisation methods

386

387 For tracking programs to be useful for practical application, digitisation accuracy must
388 be comparable to manual digitisation, as error in position data can inflate error in the
389 calculations of kinematic variables.³⁰ Image processing algorithms have been used to
390 automatically track light emitting diodes (LEDs) fixed to a swimmer's wrist in 2D video of
391 dive starts.³¹ Though the algorithm used by Slawson et al³¹ allowed high digitisation processing
392 speeds of the wrist, the estimation error was 50mm against the manually-derived wrist dive
393 trajectory. The landmark position error in our study compared with manual digitisation was
394 much lower (RMSE~4-5mm) than that of Slawson et al³¹ and compares well with the error in
395 landmark error from a markerless image processing system (wrist joint RMSE<5.6mm)
396 designed by Ceseracciu et al.³² Horizontal velocity RMSE was slightly lower in our study
397 (≤ 0.10 m/s) than wrist horizontal velocity RMSE in the study by Ceseracciu et al³² (0.17m/s).
398 Despite its relatively low error for wrist position and velocity, the markerless analysis system
399 used by Ceseracciu and et al³² had a runtime of 2-3hours to track the trajectories of three body
400 landmarks for a single front crawl trial. In addition to its processing time, the system required
401 clear images of the swimmer's silhouette during front crawl trials as well as static dry-land
402 images, which may not be feasible for sport scientists and coaches to obtain. Another automatic
403 tracking software showed excellent agreement with manual digitisation of LEDs attached to
404 the anterior superior iliac spine during front crawl swimming, with a small standard
405 measurement error of 1mm.² Following automatic digitisation, however, this tracking system
406 tended to require manual adjustments to digitised data as the tracking software on its own has
407 been found to incorrectly label between 14%² and 17%²⁹ of body landmarks. Therefore, the
408 small digitising error of 1mm using this method may be partly attributable to corrective manual
409 intervention.

410 To our knowledge, the current study is only the second application of DeepLabCutTM
411 in an aquatic setting. 2D joint position data have also been obtained using DeepLabCutTM

412 during underwater running, where the training digitisation error (neural network versus manual
413 digitisation) was ~10mm.⁹ The greater accuracy in our application of DeepLabCut™ than in
414 the underwater running study may be due to different movement patterns and/or the use of
415 black body paint to indicate joint positions in our study compared with a markerless approach
416 used by Cronin et al.⁹ Depending on the direction of the digitisation error in the 2D axis, our
417 findings could be limited by propagation error. For example, if the shoulder was digitised 5mm
418 above its true location and the hip 5mm below its location along the y-axis, hip and trunk
419 incline angles would be affected. Despite the risk of propagation error, the relative error in
420 instantaneous hip and trunk incline angles was arguably small (3.5-3.7%). Propagation error
421 would also affect horizontal velocity calculations, as digitisation error is amplified with each
422 derivative.¹⁵ The NN was accurate in determining instantaneous velocities for all three
423 landmarks when compared with manually derived velocities (Table 2). By comparison, mean
424 differences in instantaneous horizontal velocity of the head, calculated from position data
425 digitised by a NN ranged from 0.02-0.03m/s for all four competitive strokes,³³ producing a
426 similar mean difference for the knee, hip and shoulder landmarks in this study (≤ 0.01 m/s).
427 While these two applications of NNs for digitisation of 2D video differed in their experimental
428 approach, NNs appear to be an effective tool for digitisation when compared with a human
429 operator. The NN in this study produced means that were consistently within the acceptable
430 range of manual digitisation for all glide performance variables, indicating there was no loss
431 of accuracy when compared with manual digitisation with a significant improvement in
432 processing time.

433 An advantage of manual digitisation over automatic tracking methods is the decision
434 by a human operator to omit markers that are subject to blurring or have been obscured. While
435 the NN assigned coordinates to body landmarks in all frames, including body landmarks that
436 were unidentifiable by the manual operator, post-hoc analysis revealed that landmarks that
437 were given probability ratings $< 95\%$ by the NN were the same ones omitted by the manual
438 operator. The process of omitting these landmarks from the NN dataset was conducted
439 manually in our study; however, this process can be automated using a simple computational
440 routine in future applications to further improve data processing time. The image feature
441 detection algorithm in the NN software appears to be robust enough to accurately determine
442 body landmarks in underwater video that it had not been exposed to during NN training.
443 Training, therefore, needs to be done just once for a given task, such as underwater gliding, for
444 the NN to be valid for future data collections. NNs can also be trained with a sample from

445 existing databases consisting of video data with painted body landmarks, unlocking the
446 potential to analyse historical datasets in a completely new way.

447

448 Applications of neural networks in swimming

449

450 The use of a NN for digitisation in this study produced small relative error in glide
451 factor values compared with manual digitisation. This finding was impressive given glide
452 factor analysis is highly sensitive to decelerations and involves fitting a logarithmic function
453 to position data. Glide factor analysis is essential to our understanding of overall glide
454 performance because it can be used to compare glide efficiency within and between swimmers
455 by ‘correcting’ for the swimmer’s glide velocity.²⁶ By correcting for velocity, factors that
456 influence glide efficiency (e.g. posture, morphology, swim attire) can be evaluated using glide
457 factor.^{13,25} Thanks to the time-efficiency of the NN trained in this study, evaluation of glide
458 efficiency and performance from 2D video analysis is now more viable for sport scientists and
459 coaches.

460

461 Limitations and future research

462

463 The study was limited by the camera shutter speed that resulted in blurring of some
464 body landmarks during the early phase of the glide when swimmers were moving at high
465 velocities. Image distortion of body landmarks at high velocities reduced digitisation accuracy
466 of the NN compared with manual digitisation (Figure 3). Cameras with higher frame rates (e.g.
467 $\geq 120\text{Hz}$), shutter speeds, and light sensitivity may reduce the amount of body landmarks
468 omitted from analysis and provide a greater number of data points for interpolation, which may
469 further improve accuracy of kinematic variable calculations.

470

471 The image recognition algorithm of the NN was found to be as accurate as a human
472 operator for digitisation of painted landmarks in video captured under the same environmental
473 conditions as the training frames. However, changes to the visual characteristics of painted
474 landmarks in 2D video may limit the ability of the NN to recognise them, as evident with
475 landmark distortion at high velocities. We were unable to assess whether digitisation accuracy
476 of this NN would occur in glide video at a different location with different lighting properties,
477 water clarity, and camera specifications, resulting in the possibility of overfitting the neural
network to the training dataset. Future research would be advantageous to determine whether

478 variability of video input in the NN training procedure improves robustness of the NN and
479 generalisability to multiple settings. While the NN required approximately nine hours to train,
480 once trained, the weights can be copied onto any local machine and used for analysis purposes
481 on a basic laptop computer.

482 Training time could have been reduced in this study by reducing the image resolution
483 of the training frames,³⁴ though it is unlikely that digitising accuracy would have been impacted
484 because the input videos had the same resolution as the training images. Calibration time was
485 negatively impacted because the camera setup required a field of view correction to minimise
486 reprojection error. Where a fixed-camera setup is not viable, cameras with minimal visual
487 distortion at the bounds of the field of view would reduce the need for a field of view correction
488 and minimise calibration time.

489 Digitisation accuracy appeared to be improved by applying black body paint to body
490 landmarks compared with markerless analysis methods.^{9,32} In regards to the NNs trained in
491 DeepLabCutTM for an aquatic setting, the use of painted landmarks improved 2D digitisation
492 error from 10mm⁹ to 4-5mm in our study. Additional time and expertise, however, is required
493 to mark swimmers. Sports scientists and coaches should consider the trade-off between
494 preparation time and accuracy when using NNs to digitise 2D video. The methods presented
495 here could be used in future research involving kinematic analysis of land-based activities,
496 especially those performed predominantly in a single plane of motion. In athletics, for instance,
497 a fixed-camera setup and pre-calibrated area could be used to assess 2D kinematics of running,
498 jumping, or throwing in a training environment. Kinematic analysis in weightlifting commonly
499 involves video and manual digitisation methods to estimate barbell trajectory during lifts.³⁵
500 Barbell trajectory can be used to assess movement characteristics, provide technical feedback,
501 and calculate critical performance variables, such as barbell velocity.³⁶ Automated digitisation
502 of the end of the barbell in 2D video, however, is difficult as it can exhibit similar colour
503 characteristics to the surrounding image.³⁷ Given the maximal barbell velocity of elite
504 weightlifters during the snatch lift is between 1.5-2m/s,^{38,39} NNs could be used for automated
505 digitisation of the barbell in the sport of weightlifting.

506

507 Conclusion

508

509 To our knowledge, few studies exist in which kinematic data from video analysis have
510 been derived in an accurate, time-efficient manner and the most effective strategies have

511 involved the use of NNs. DeepLabCut™ was found to be an accurate method of extracting
512 kinematic data to analyse glide posture, efficiency and performance compared with manual
513 digitisation. The use of NN software for auto-digitisation of body landmarks could be
514 substantially beneficial to biomechanics researchers, sports scientists, and coaches. The time
515 saving compared to manual digitising may enable rapid feedback of performance measures in
516 training and simulated-competitive environments.

517

518 Disclosure of interest

519

520 The authors report no conflict of interest.

521 References

522

- 523 1. Yeadon M, Challis JH. The future of performance-related sports biomechanics
524 research. *J Sport Sci.* 1994;12(1):3-32.
- 525 2. Dos Santos KB, Lara JP, Rodacki AL. Reproducibility and repeatability of intracyclic
526 velocity variation in front crawl swimming from manual and semi-automatic
527 measurement. *Human Movement.* 2017;18(3):55-59.
- 528 3. Adnan NMN, Ab Patar MNA, Lee H, Yamamoto SI, Jong-Young L, Mahmud J.
529 Biomechanical analysis using Kinovea for sports application. *IOP Conference Series:
530 Materials Science and Engineering.* 2018;342(1):012097.
- 531 4. Mathis A, Mamidanna P, Cury KM, et al. DeepLabCut: markerless pose estimation of
532 user-defined body parts with deep learning. *Nature neuroscience.* 2018;21(9):1281.
- 533 5. Mehrizi R, Peng X, Xu X, Zhang S, Li K. A Deep Neural Network-based method for
534 estimation of 3D lifting motions. *Journal of biomechanics.* 2019;84:87-93.
- 535 6. Pishchulin L, Insafutdinov E, Tang S, et al. Deepcut: Joint subset partition and labeling
536 for multi person pose estimation. *Proceedings of the IEEE conference on computer
537 vision and pattern recognition.* 2016:4929-4937.
- 538 7. Insafutdinov E, Pishchulin L, Andres B, Andriluka M, Schiele B. Deepercut: A deeper,
539 stronger, and faster multi-person pose estimation model. *European Conference on
540 Computer Vision.* 2016:34-50.
- 541 8. Sanders RH, Gonjo T, McCabe CB. Reliability of three-dimensional linear kinematics
542 and kinetics of swimming derived from digitized video at 25 and 50 Hz with 10 and 5

- 543 frame extensions to the 4th order Butterworth smoothing window. *Journal of sports*
544 *science & medicine*. 2015;14(2):441.
- 545 9. Cronin NJ, Rantalainen T, Ahtiainen JP, Hynynen E, Waller B. Markerless 2D
546 kinematic analysis of underwater running: A deep learning approach. *Journal of*
547 *biomechanics*. 2019;87:75-82.
- 548 10. Stamm A, James DA, Burkett BB, Hagem RM, Thiel DV. Determining maximum push-
549 off velocity in swimming using accelerometers. *Procedia Engineering*. 2013;60:201-
550 207.
- 551 11. Guimaraes AC, Hay JG. A mechanical analysis of the grab starting technique in
552 swimming. *Journal of Applied Biomechanics*. 1985;1(1):25-35.
- 553 12. Cossor J, Mason B. Swim start performances at the Sydney 2000 Olympic Games.
554 *Proceedings of Swim Sessions of the XIX Symposium on Biomechanics in Sports*
555 2001:70–74.
- 556 13. Naemi R, Psycharakis SG, McCabe C, Connaboy C, Sanders RH. Relationships
557 between glide efficiency and swimmers' size and shape characteristics. *Journal of*
558 *applied biomechanics*. 2012;28(4):400-411.
- 559 14. Zamparo P, Gatta G, Pendergast D, Capelli C. Active and passive drag: the role of trunk
560 incline. *Eur J Appl Physiol*. 2009;106(2):195-205.
- 561 15. Winter DA. *Biomechanics and motor control of human movement*. Hoboken, New
562 Jersey: John Wiley & Sons; 2009.
- 563 16. McCabe CB, Psycharakis S, Sanders R. Kinematic differences between front crawl
564 sprint and distance swimmers at sprint pace. *Journal of Sports Sciences*.
565 2011;29(2):115-123.
- 566 17. Naemi R, Easson WJ, Sanders RH. Hydrodynamic glide efficiency in swimming.
567 *Journal of Science and Medicine in Sport*. 2010;13(4):444-451.
- 568 18. Elipot M, Dietrich G, Hellard P, Houel N. Poster Session II, July 14th 2010—Abstracts:
569 Cinalysis: A new software for swimming races analysis. *Procedia Engineering*.
570 2010;2(2):3467.
- 571 19. Bouguet J-Y. Camera calibration toolbox for Matlab (2008). URL
572 [http://www.visioncaltechedu/bouguetj/calib_doc/](http://www.vision.caltech.edu/bouguetj/calib_doc/). 2008;1080.
- 573 20. Zhang Z. A flexible new technique for camera calibration. *IEEE Transactions on*
574 *pattern analysis and machine intelligence*. 2000;22(11):1330-1334.
- 575 21. Abdel-Aziz Y, Karara H. Direct linear transformation into object space coordinates in
576 close-range photogrammetry. *Proc Symp Close-Range Photogrammetry*. 1971:1-18.

- 577 22. Kwon YH, Casebolt JB. Effects of light refraction on the accuracy of camera calibration
578 and reconstruction in underwater motion analysis. *Sports biomechanics*. 2006;5(2):315-
579 340.
- 580 23. He K, Zhang X, Ren S, Sun J. Deep residual learning for image recognition.
581 *Proceedings of the IEEE conference on computer vision and pattern recognition*.
582 2016:770-778.
- 583 24. Pishchulin L, Insafutdinov E, Tang S, et al. Deepcut: Joint subset partition and labeling
584 for multi person pose estimation. Paper presented at: Proceedings of the IEEE
585 conference on computer vision and pattern recognition2016.
- 586 25. Naemi R, Sanders RH. A “hydrokinematic” method of measuring the glide efficiency
587 of a human swimmer. *Journal of biomechanical engineering*. 2008;130(6).
- 588 26. Machtsiras G. *Utilizing Flow Characteristics to Increase Performance in Swimming*
589 *(Unpublished doctoral dissertation)*. Edinburgh, Scotland The University of
590 Edinburgh; 2012.
- 591 27. Koo TK, Li MY. A guideline of selecting and reporting intraclass correlation
592 coefficients for reliability research. *Journal of chiropractic medicine*. 2016;15(2):155-
593 163.
- 594 28. Thow JL, Naemi R, Sanders RH. Comparison of modes of feedback on glide
595 performance in swimming. *J Sport Sci*. 2012;30(1):43-52.
- 596 29. Magalhaes FA, Sawacha Z, Di Michele R, Cortesi M, Gatta G, Fantozzi S.
597 Effectiveness of an automatic tracking software in underwater motion analysis. *Journal*
598 *of sports science & medicine*. 2013;12(4):660.
- 599 30. Robertson G, Caldwell G, Hamill J, Kamen G, Whittlesey S. *Research methods in*
600 *biomechanics*. 2 ed. Champaign, IL: Human Kinetics; 2013.
- 601 31. Slawson S, Conway P, Justham L, West A. The development of an inexpensive passive
602 marker system for the analysis of starts and turns in swimming. *Procedia Engineering*.
603 2010;2(2):2727-2733.
- 604 32. Ceseracciu E, Sawacha Z, Fantozzi S, et al. Markerless analysis of front crawl
605 swimming. *Journal of biomechanics*. 2011;44(12):2236-2242.
- 606 33. Elipot M. A new paradigm to do and understand the race analyses in swimming: The
607 application of convolutional neural networks. *ISBS Proceedings Archive*.
608 2019;37(1):455.
- 609 34. Mathis A, Warren RA. On the inference speed and video-compression robustness of
610 DeepLabCut. *BioRxiv*. 2018:457242.

- 611 35. Garhammer J. Biomechanical profiles of Olympic weightlifters. *Journal of Applied*
612 *Biomechanics*. 1985;1(2):122-130.
- 613 36. Garhammer J, Newton H. Applied video analysis for coaches: Weightlifting examples.
614 *International Journal of Sports Science & Coaching*. 2013;8(3):581-594.
- 615 37. Dæhlin TE, Krosshaug T, Chiu LZ. Enhancing digital video analysis of bar kinematics
616 in weightlifting: A case study. *The Journal of Strength & Conditioning Research*.
617 2017;31(6):1592-1600.
- 618 38. Nagao H, Kubo Y, Tsuno T, Kurosaka S, Muto M. A Biomechanical Comparison of
619 Successful and Unsuccessful Snatch Attempts among Elite Male Weightlifters. *Sports*.
620 2019;7(6):151.
- 621 39. Gourgoulis V, Aggeloussis N, Garas A, Mavromatis G. Unsuccessful vs. successful
622 performance in snatch lifts: a kinematic approach. *The Journal of Strength &*
623 *Conditioning Research*. 2009;23(2):486-494.
- 624